Effect of cold rolling on microstructure and mechanical properties of copper subjected to ECAP with various numbers of passes

N.D. Stepanov, A.V. Kuznetsov, G.A. Salishchev, G.I. Raab, R.Z. Valiev

A B S T R A C T

Microstructure and mechanical properties of copper subjected to 1–10 ECAP passes via route B_c were compared with those for further cold rolled specimens. Microstructure was studied by means of TEM and EBSD analysis in three orthogonal sections. Rolling caused transformation of reasonably equiaxed structure after ECAP into lamellar one due to geometrical effect of deformation, but almost no additional grain refinement occurred during rolling. Significantly higher extent of HABs (about 20% irrespectively to passes number) was found after rolling. This was associated with more pronounced dynamic restoration process during rolling. Mechanical properties were estimated by tension testing at room temperature. Yield strength increased by $\sim$100 MPa after rolling due to finer boundary spacing according to Hall–Petch relationship.

Keywords:
Copper
ECAP
Cold rolling
Microstructure refinement
Dynamic restoration
Mechanical properties

1. Introduction

Ultra-fine grained (UFG) materials were subject of great interest during recent years due to their outstanding mechanical properties. One of the possible ways of producing UFG materials is application of severe plastic deformation (SPD) [1]. Numerous SPD methods were proposed, among them equal angular channel pressing (ECAP) [2] and high-pressure torsion (HPT) [3] are the most developed ones. They allow producing bulk fully-dense materials with highly-refined structure.

Almost unlimited strain could be imposed by SPD methods but grain refinement and related strengthening are evident only at low or moderate strains, after that saturation stage is reached [4]. So microstructure could not be refined beyond a certain level. Further grain refinement and enhancement of strength could be obtained by additional deformation treatment. For instance, combination of ECAP and rolling was used for different materials, including copper and its alloys [5–7], aluminum alloys [8–11], IF-steel [12] and titanium [13,14]; increase in strength and refined structure were often reported. This type of treatment is especially interesting as it could have some industrial application in producing sheets with UFG structure. However, it is not still clear yet, what is the exact mechanism (or mechanisms) of structure evolution during rolling of as-ECAPed materials. This question is especially challenging as in most studies material is already prestrained by ECAP up to saturation of microstructure refinement. Change of deformation mode from ECAP to rolling could initiate new dislocation slip systems in accordance with change in stress–strain state and/or decrease boundary spacing according to geometrical requirements of strain.

To study evolution of structure during deformation usually some treatment conditions are changed and their effect on structure is considered. In case of ECAP combined with rolling both ECAP and rolling conditions could be changed. For instance, effect of rolling thickness reduction (or strain) after ECAP was studied by Hazra et al. [12], effect of temperature and strain during plane-strain compression was studied by Prangnell [9]. ECAP conditions received much less attention. Effect of strain imposed by ECAP prior to rolling (e.g. passes number) was studied by El-Danaf [10,11], but there main emphasis was made on texture evolution. There is evident lack of information on correlation between passes number and microstructure and properties after rolling. Thus in current study we performed detailed investigation of microstructure and mechanical properties of copper subjected to ECAP with different number of passes and subsequent cold rolling. Copper was chosen due to two reasons: at first, microstructure and properties of copper after ECAP were extensively studied [14–18], and second, limited attempts [5–7] were made to investigate microstructure and properties development of copper after ECAP and rolling. The main aim was to provide further understanding in how microstructure develops when deformation mode is changed at large strains and how microstructure influences mechanical properties.

2. Experimental procedures

Commercial purity copper (99.953 wt.% Cu, 0.0095 wt.% O_2) was used in present study. It was supplied in rod with dimensions ⌀ 30 mm × 2500 mm. Initial microstructure consisted from elongated grains with average size about 200 μm. Many annealing twins were observed. For ECAP rods with dimensions ⌀ 25 mm × 120 mm were used. ECAP was conducted at room temperature using a die with a channel angle 90° at 5 mm/s ram speed. Rods were pressed via route B_c, number of passes varied from 1 to 10. After ECAP rods were cut in two halves and one of the half from each rod was machined to obtain two opposite flat surfaces. Distance between these surfaces (thickness) was 15 mm. These billets were subjected to cold sheet rolling with thickness reduction about 5–10% per pass. We performed FEM analysis (DEFORM 3D software was used) to evaluate temperature rise due to deformation heating, and the results showed that the temperature in the midthickness of the specimens rose to about 50 °C during ECAP, and only to about 30 °C during rolling. Between the passes billets were cooled on air to minimize an influence of deformation heating on microstructure. Final thickness was equal to 1.5 mm and total thickness reduction was 90%. Rolling direction was perpendicular to extrusion direction. In order to adequately compare strain imposed during ECAP and rolling we used equivalent (Von Mieses) strain. Equivalent strain per one ECAP pass was equal to 1.15, and rolling imposed strain of 2.7. For microstructure analysis of as-ECAPed samples parallelepipeds with cross-section about 10 mm × 10 mm were cut from central part of the billets. Microstructure was examined in three orthogonal planes, each of them was perpendicular to ED, TD and ND direction respectively (see Fig. 1a). Planes would be named according to their perpendicular direction further, i.e. plane perpendicular to ED direction is going to be named ED plane. Similar scheme was applied for rolled samples (Fig. 1b), and planes would be named further in the same fashion. All examination was performed approximately at the middle of thickness. Thin foils for TEM were prepared using conventional electropolishing method. JEOL JEM-2100 operating at 200 kV was used for observations. At least 4 bright-field images with magnification ×40000 were taken in order to calculate size of grains/subgrains by standard linear interception method. No distinction between different structural elements (grains, subgrains) was made and simply smallest ones were measured. In case of non-equiaxed structure measurements were made along short axis (i.e. "thickness" was measured).

For electron-backscattered diffraction (EBSD) analysis was used FEI Quanta 600 field-emission gun scanning electron microscope (FEG-SEM). Prior to EBSD analysis samples were carefully polished mechanically and then electropolished. Usually scans were taken at magnification ×8000 and beam parameters 20 kV and 18 nA. Typical scan area was 30 μm × 30 μm with step size equal to 65 nm. EBSD data was processed with TSL OIM^{TM} version 5.2 software. Low-angle boundaries (LABs) ($2° \leq \theta < 15°$) and high-angle boundaries (HABs) ($\theta \geq 15°$) are shown on EBSD maps with white and black lines respectively. From EBSD maps LABs/HABs spacing was measured by standard linear interception method. For non-equiaxed structure measurements were made similarly to TEM measurements. Structural elements having only HABs were considered as grains. Those which had only LABs or both LABs and HABs were considered as subgrains.

Tensile tests were performed on samples with gauge dimensions 1.5 mm × 3 mm × 16 mm. Samples were cut from central part of ECAPed billets and rolled sheets parallel to extrusion/rolling direction. Testing was performed with Instron 5882 testing machine at room temperature, 3 samples were tested for each state. Initial strain rate was $\sim 10^{-1}\,s^{-1}$.

3. Results

3.1. Microstructure

TEM investigation showed that elongated subgrain structure was formed after 1 ECAP pass (Fig. 2a). Most of the boundaries were curved, thick and fuzzy. This appearance could be attributed to their low-angle misorientation. On ED and TD planes boundaries were aligned parallel to ND plane, and on ND plane no preferred orientation of boundaries was found. After 2 passes (Fig. 2c) structure became rather equiaxed but still majority of the boundaries had low-angle appearance. After 4 and 10 passes (Fig. 2e and g) microstructure had similar features. However, boundaries appeared thinner and sharper possibly due to increase of their misorientation and grains/subgrains had more regular shape. Both equiaxed and elongated grains/subgrains were found after 4 and 10 passes. Elongated grains were observed on ED and TD planes after 4 passes and only on TD plane after 10 passes. These grains had well-defined preferred orientation (in metallographic terms) and were oriented in accordance with shear direction. The difference between microstructure on different planes was not significant, especially after 4 and 10 passes.

Rolling caused serious changes in microstructure (Fig. 2b, d, f and h), it became significantly different in ND and RD/TD planes. On the ND plane structure was rather equiaxed, boundaries were curved and diffusively scattered. In contrast on RD and TD planes very fine lamellar structure was observed. Lamellar boundaries were usually straight and looked sharp. Many lamellae were subdivided by thick transversal boundaries.

Interesting microstructural feature of copper after ECAP and rolling was presence of defect free-grains structure after 4 and especially 10 passes and rolling. An example of such structure is shown in Fig. 3. These grains were inclined into lamellar structure and usually were situated "inside" lamellar structure. They had sharp boundaries and low aspect ratio contrasting with elongated

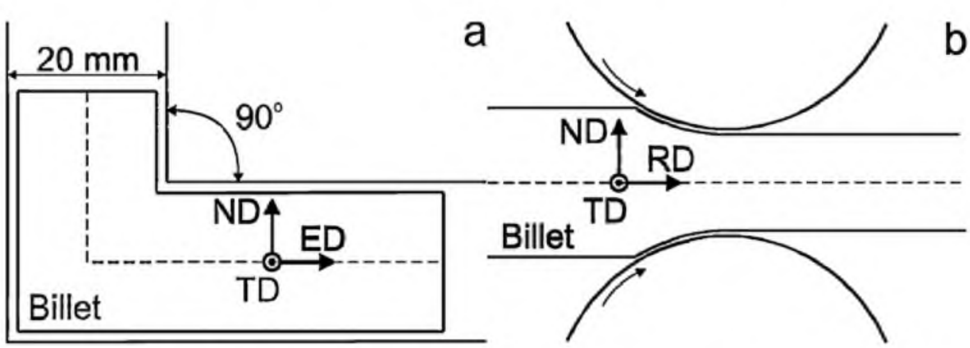

Fig. 1. Schematic representation of (a) ECAP billet with three orthogonal directions, (b) ECAP and cold rolled billet with three orthogonal directions.

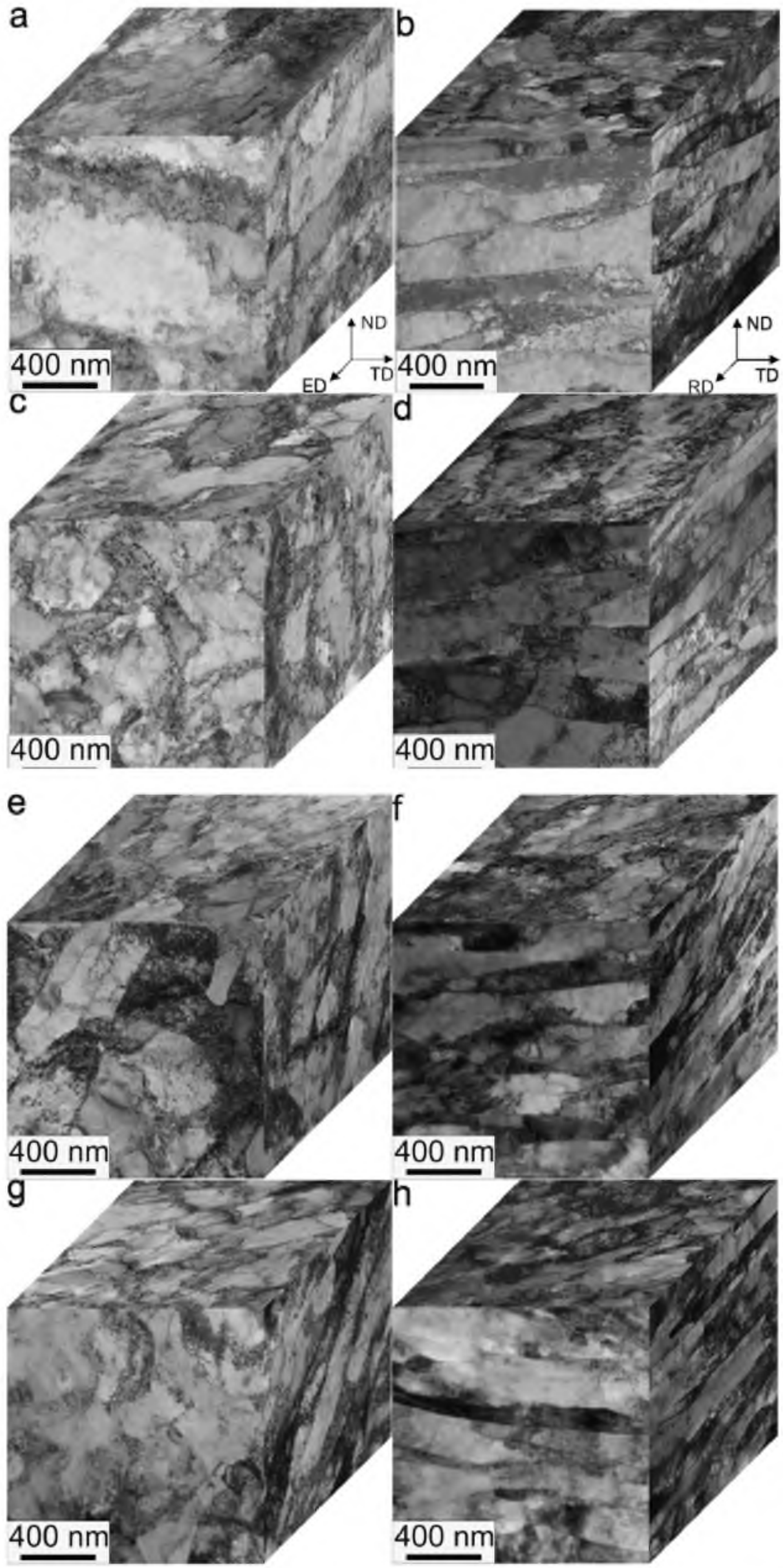

Fig. 2. TEM images of copper processed by ECAP (a, c, e, g) and ECAP with susequent rolling (b, d, f, h) with different passes number: a, b – 1, c, d – 2, e, f – 4, g, h – 10.

lamellae. We could not find similar grains after ECAP despite thorough observations.

Values of boundary spacing are shown in Fig. 4. It is clear that in both cases – ECAP and ECAP with subsequent rolling – increase in passes number resulted in decrease in values of boundary spacing in similar manner. For ECAP this decrease was mostly pronounced after first two passes and less significant after 4 and more passes (Fig. 4a). Boundary spacing was very similar on all planes

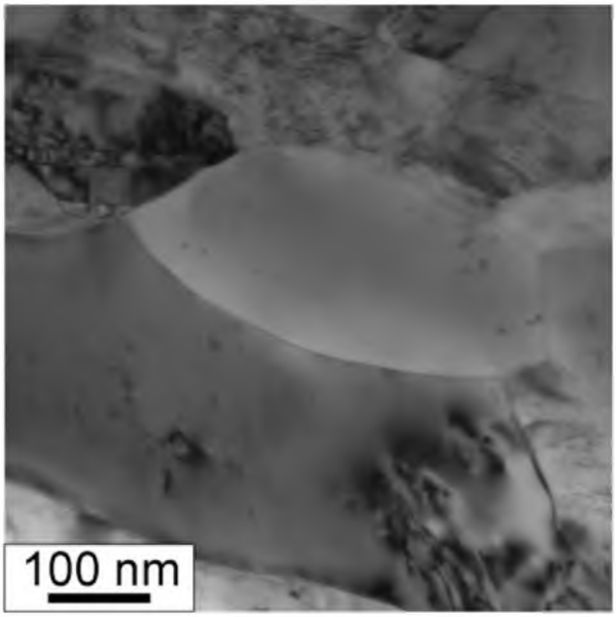

Fig. 3. TEM image of copper after 10 ECAP passes and subsequent rolling (TD plane).

(difference is within margin of error). Boundary spacing achieved by means of ECAP was about 180 nm after 10 passes. It was mentioned previously that after rolling microstructure was different on ND and RD/TD planes and it is mirrored in Fig. 4b. On ND plane boundary spacing after rolling decreased gradually with increase in strain and its value was similar to those for ECAP. On RD/TD planes spacing is significantly lower. Its value is about 110–130 nm after 2–10 passes and ECAP. Only slight decrease in spacing after first two passes was found.

EBSD misorientation maps of copper after ECAP and ECAP with subsequent rolling are shown in Fig. 5. After 1 and 2 ECAP (Fig. 5a and c) passes structure predominantly consisted from mostly elongated subgrains. Insignificant number of elongated grains was found (Fig. 5a, TD plane for example). Some of the elongated grains/subgrains were oriented in accordance with shear direction. These oriented grains/subgrains were found on ED plane and partially on TD plane after 2 passes. After 4 passes (Fig. 5e) metallographic texture was more prominent and preferred orientation was found on all planes. But alongside with elongated grains/subgrains equiaxed ones existed. Many fine submicron-sized grains (surrounded by HABs) were observed. Some of them were subdivided into subgrains by LABs. In general, equiaxed grains were finer and often free of LABs comparing to elongated ones. After 10 ECAP passes structure also became much more equiaxed, clear metallographic texture is seen only on TD plane. However, even after 10 passes areas with mostly LABs existed. Structure could be treated as very inhomogeneous. Except for metallographic texture no significant difference between microstructure on different planes was found.

EBSD analysis of rolled specimens (Fig. 5b, d, f and h) is rather consistent with TEM observations. On ND plane microstructures resembled much those after ECAP with corresponding number of passes. This structure was inhomogeneous, with both fine grains and areas comprising mostly subgrains. Character of microstructure on ND plane has not changed as number of passes increased. On RD and TD planes lamellar structure was found. After first two passes structure was highly inhomogeneous, longitudinal boundaries had both low- and high-angle misorientations. Increase in ECAP passes resulted in homogeneous structure with mostly high-angle longitudinal boundaries. Transversal boundaries had mostly low-angle misorientation without respect to passes number. Also some equiaxed grains were found mainly on RD plane. On TD plane shear bands are clearly seen (Fig. 5d, in upper corner of TD - for example).

Spacing between HABs (Fig. 6a and c) and LABs (Fig. 6b and d) calculated from EBSD maps as a function of ECAP passes number was plotted for ECAP (Fig. 6a and b) and ECAP with subsequent rolling (Fig. 6c and d). Dependence for HABs spacing after ECAP (Fig. 6a) requires some comments. As only small fraction of fine grains was found after 1 and 2 passes, no values are given for 1 pass because number of grains on maps was not sufficient to provide any statistically reliable data. Values for 2 passes are given, but they are not included in the plot. After 4 and 10 pass prominent grain structure was formed and average grain size reduced with increase in strain. After 10 ECAP passes average HABs spacing is ~0.6–0.7 μm. LABs spacing decreased gradually during ECAP up to ~0.4 μm after 4 passes (Fig. 6c). Additional ECAP straining does not result in further reduction of spacing. For ECAP there was no meaningful difference between both HABs and LABs spacing values on different planes. But after rolling there was significant difference in evolution of microstructural parameters on different planes (Fig. 6b and d). On ND plane both HABs and LABs spacing reduced slightly after first two passes and reached saturation at values about ~0.9 μm for HABs spacing and ~0.6 μm for LABs spacing. On RD and TD planes spacing between boundaries decreased gradually with increase in passes number. Values of spacing on these two planes

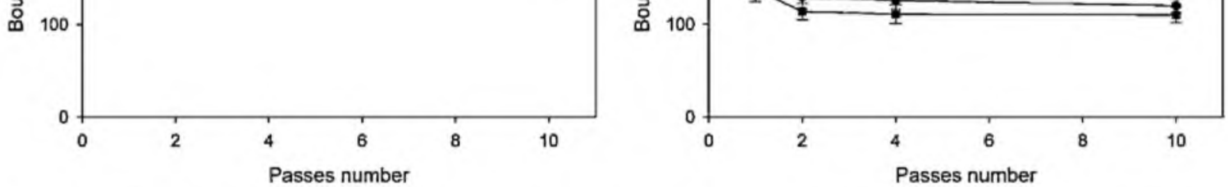

Fig. 4. Dependence of boundary spacing on different planes on ECAP passes number for copper after ECAP (a) and ECAP with subsequent rolling (b).

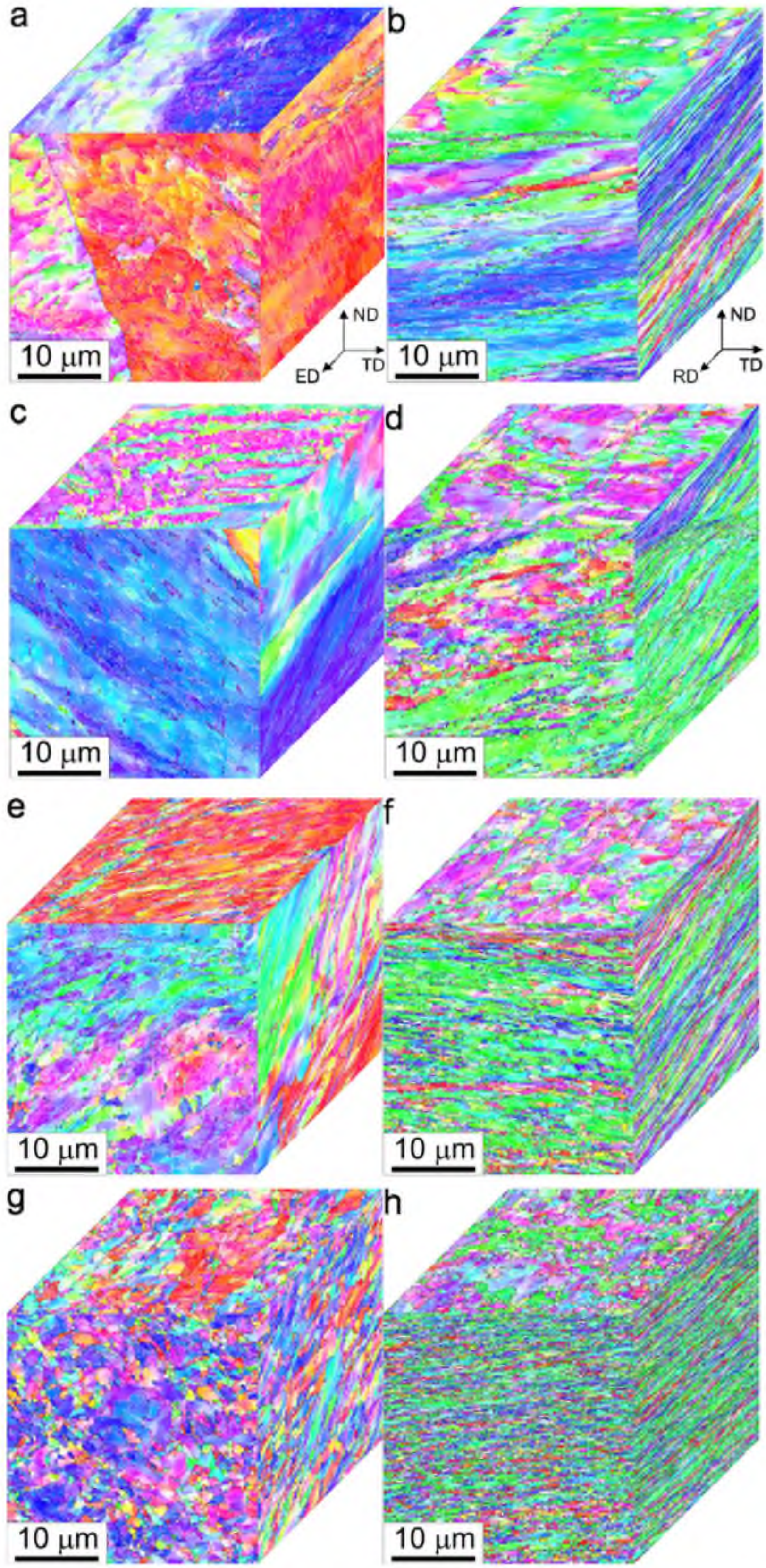

Fig. 5. EBSD orientation maps of copper after ECAP (a, c, e, g) and ECAP with subsequent rolling (b, d, f, h); a, b – 1 pass; c, d – 2 passes; e, f – 4 passes; g, h – 10 passes.

became close at high strain and are equal to ~0.3 μm for both HABs and LABs.

Data on HABs fraction is given in Table 1. It is clearly seen that average HABs fraction (mean of values obtained for different planes) increased with increase in passes number both for ECAP and ECAP with subsequent cold rolling. Rate of average HABs fraction increase was quite similar – about 30% difference between 1 and 10 passes for both ECAP and ECAP with subsequent cold rolling.

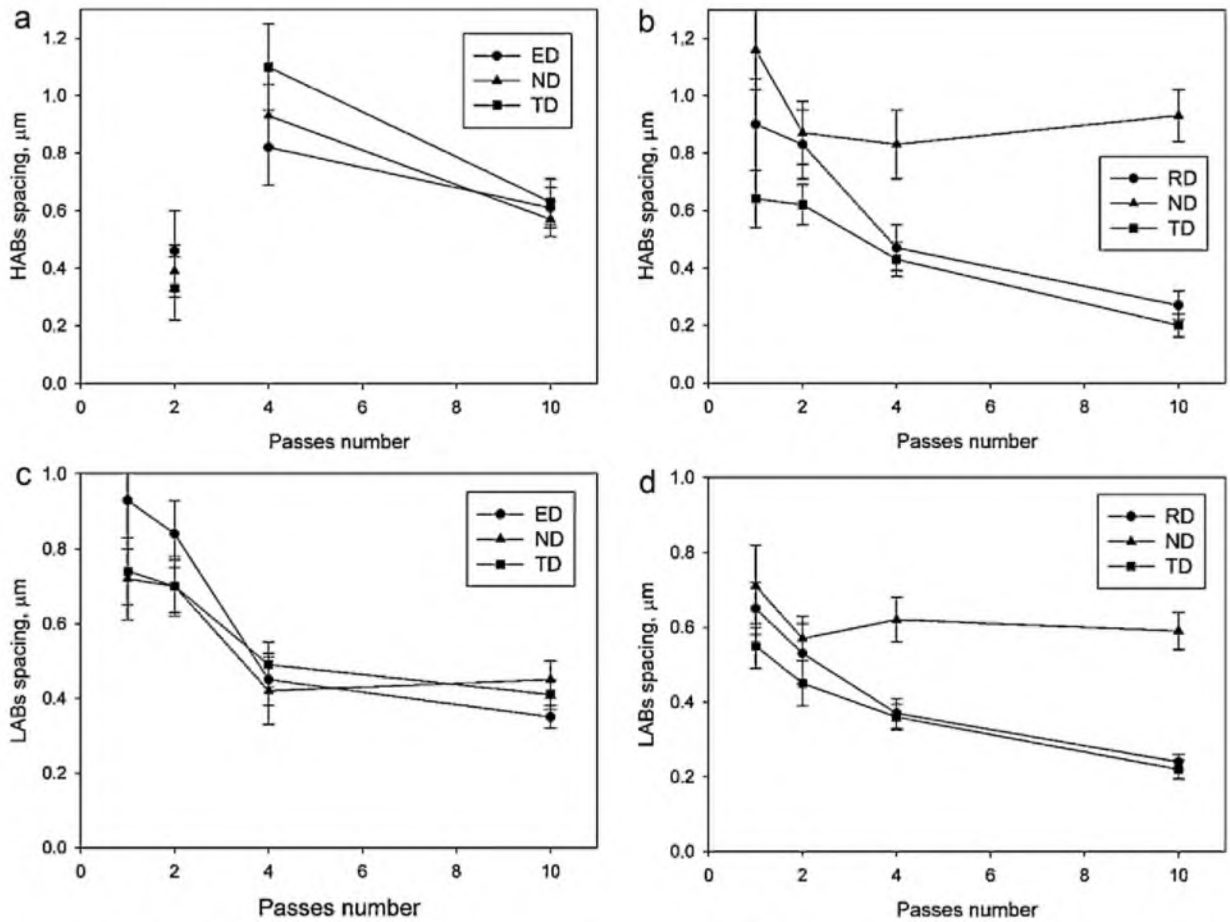

Fig. 6. Dependence of boundary spacing on different planes on ECAP passes number for copper after ECAP (a, c) and ECAP with subsequent rolling (b, d): a, b – HABs, c, d – LABs.

But rolling after ECAP significantly increased average HABs fraction – from 9.2% to 31.1% after 1 pass and from 40.0% to 62.0% after 10 passes. Average HABs fraction increment was approximately equal to 20% for all passes numbers. Variation between HABs fraction on different planes was not so significant in case of ECAP – values differed from average value not higher than by ~5%; only after 2 passes variation between HABs fraction on different planes was higher. Variations of HABs fraction could be attributed to heterogeneity of microstructure produced by ECAP. After rolling HABs fraction was similar on RD and TD planes and its value was much higher than those on ND plane.

Pole figures were also derived from EBSD data. Complex shear texture with rotation about 45° around its axis was found after ECAP. This type of texture was well anticipated after ECAP [19]. Some deviations from expected orientations were found possibly due to inhomogeneous plastic flow. After rolling texture transforms into typical rolling texture, with two distinctive preferred orientations – copper {1 1 2} ⟨1 1 1⟩ and S {1 2 3} ⟨6 3 4⟩. Transition from ECAP texture to rolling texture after rolling with 90% reduction correlates well with previous results for IF-steel [12]. Both rolling and ECAP textures were extensively studied before and as our results were rather typical they are not going to be discussed further.

Table 1
HABs fraction (%) in copper after ECAP and ECAP with subsequent cold rolling depending on passes number, separate values for each plane are given as well as average.

Plane	Passes number			
	1	2	4	10
	ECAP			
ED	11.3	14.9	20.5	46.4
ND	12.9	8.7	23.3	38.3
TD	5.3	22.8	28.6	36.0
Average	9.2	14.3	23.9	40.0
	ECAP + rolling			
RD	24.5	42.2	54.2	71.1
ND	25.5	25.2	29.7	45.4
TD	42.8	40.9	57.7	74.0
Average	31.1	35.2	45.3	62.0

3.2. Mechanical properties

Data on mechanical properties is summarized in Table 2. Ultimate tensile strength (U.T.S.) and yield strength (Y.S.) values showcased similar dependence on passes number for both

Table 2
Mechanical properties of copper after ECAP and ECAP with subsequent rolling.

Passes number	1	2	4	10
ECAP				
U.T.S. (MPa)	318 ± 17	365 ± 9	394 ± 13	402 ± 11
Y.S. (MPa)	299 ± 26	350 ± 12	347 ± 18	348 ± 15
e_u, %	1.3 ± 0.2	0.9 ± 0.3	1.1 ± 0.2	2.1 ± 0.5
e_t, %	11.7 ± 1.6	11.7 ± 1.1	10 ± 1.5	12.7 ± 0.9
ECAP + rolling				
U.T.S. (MPa)	433 ± 12	461 ± 15	480 ± 14	485 ± 14
Y.S. (MPa)	425 ± 19	446 ± 23	450 ± 18	462 ± 16
e_u, %	0.9 ± 0.2	1.6 ± 0.3	3.0 ± 0.4	2.8 ± 0.3
e_t, %	8.9 ± 1.3	11.1 ± 1.9	14.3 ± 1.0	13.8 ± 0.7

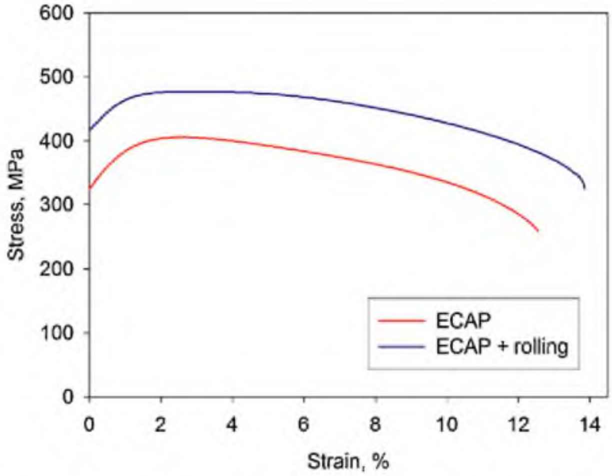

Fig. 7. Stress–strain curves after ECAP (10 passes) and ECAP with subsequent cold rolling.

ECAP and ECAP with subsequent rolling. U.T.S. increased gradually when passes number rises from 1 to 4 and reached saturation after 4th pass. Y.S. reaches saturation already after 2 passes. Rolling increased U.T.S. approximately by 80–100 MPa and Y.S. by 100–130 MPa depending on passes number. No dependence of both uniform elongation (e_u) and total elongation (e_t) on processing strain was found for ECAP. They remained almost constant in range 1–2% for e_u and 10–13% for e_t approximately. After rolling elongation increased with increase in ECAP passes number from 1 to 4, and after that stayed unchanged. Maximum values (after 4 and 10 ECAP passes and rolling) were about 3% for e_u and 14% for e_t.

Two stress–strain curves – after 10 ECAP passes and 10 passes with subsequent rolling – are shown as an example in Fig. 7. The higher peak stress values were found after rolling as it was expected from higher strength values from Table 2. After reaching maximum value stress decreased slower after rolling and a more extended steady-state stage was observed after rolling. These factors resulted in slightly higher ductility.

4. Discussion

4.1. Microstructure

Structural observations showcase that rolling causes dramatic changes in microstructure. Previously equiaxed or elongated in shear direction grains/subgrains, typical for ECAP [20–22], became flattened in accordance with thickness reduction caused by rolling deformation. Their appearance resembles pancakes elongated in rolling direction. Strong metallographic texture develops as a result of flattening and realignment of initial structure. As a result elongated structure with lamellar boundaries perpendicular to ND was found on RD and TD planes after rolling. TEM revealed that distance between lamellar boundaries demonstrate rather week dependence on ECAP passes number, i.e. strain imposed before rolling. However, spacing between lamellar HABs obtained by EBSD decreases significantly with increase in ECAP passes number. It indicates that lamellar boundaries do not always have high-angle misorientation and their misorientation increases with strain imposed by ECAP. Rather equiaxed structure is seen on ND plane with much lower fraction of HABs than on RD/TD planes. It should be mentioned that very similar findings about difference of microstructure on different planes were made on Al alloy after ECAP and plane strain compression [11].

In general, observed microstructure resembles typical microstructure of heavily rolled cubic metals [23]. It indicates that rolling with 90% reduction completely transforms as-ECAPed microstructure to rolling-type structure. This structure could be described in terms of geometrically necessary boundaries (GNBs) and incidental dislocation boundaries (IDBs). GNBs are lamellar boundaries in case of rolling. Lamella usually is subdivided into several fragments by transversal IDBs. GNBs have much higher misorientation than IDBs, although they are not necessary HABs. GNBs are aligned almost parallel to ND plane and IDBs have to be perpendicular to ND plane with highly possible deviations. On our images one has to observe GNBs with IDBs on RD/TD planes and almost only IDBs on ND plane. As a result, lamellar structure is observed on RD/TD planes, on ND structure is rather equiaxed. Also, higher fraction of HABs on RD/TD planes is anticipated because as only GNBs could have high-angle misorientation.

During ECAP saturation of grain refinement is reached already after 2 or 4 ECAP passes (according to TEM or EBSD data respectively). It seems reasonable that saturation size equal to approximately 180 nm (indicated by TEM) is minimal grain/subgrain size achievable in copper by plastic deformation, at least, at room temperature. Application of even very high strains, by means of ECAP or HPT results in grain size about 200 nm in copper [14,24]. Also the difference between saturation value and grain/subgrain size after first pass (~300 nm) is not that significant. It means that further refinement during plastic straining would not result in significant grain/subgrain size decrease even after 1 ECAP pass. However, from Figs. 4 and 6a and b it is clearly seen that grain/subgrain thickness and LABs spacing decreases significantly after rolling. This fact is highly possible related with geometrical effect of rolling straining [25]. According to geometrical consideration each grain should change its shape like the whole specimen. That is the reason why grains/subgrains obtain typical pancake shape after rolling. This also causes decrease in boundaries spacing on RD and TD planes. But on ND plane spacing between boundaries and grain/subgrain size could be similar or even higher than they were before rolling. So, the question is what process governs microstructure development during rolling: change of grains/subgrains shape according to geometrical requirements of strain or further grain refinement.

Grain refinement due to fragmentation of initial structure, as it mostly happens during SPD at ambient temperatures, involves creation of new boundaries. This should cause pronounced increase in density of the boundaries (area of the boundaries in specific volume related to the volume, S/V). However, if the microstructure evolves in accordance with geometrical effect of strain, no new boundaries are created and the boundary density does not increase that significantly. So boundary density could be used to distinguish grain refinement from geometrical effect of strain. To evaluate boundaries density we used simple equation for surface to volume ratio of partly oriented structures [25]:

$$\frac{S}{V} = \frac{1}{d_{\mathrm{ND}}} + \frac{0.429}{d_{\mathrm{ED/RD}}} + \frac{0.571}{d_{\mathrm{TD}}}$$

d_i where i is ND, ED/RD or TD grain size on corresponding plane.

Values of boundary density calculated from TEM data are plotted against total equivalent strain in Fig. 8. It is clearly seen that density of boundaries follows one and the same dependence on equivalent strain for ECAP and ECAP with rolling. Strain has the accumulative effect on boundary density without regard to deformation mode. Two stages are distinguished in the dependence: rapid rise of boundary density in the beginning and slight increase during following straining. Transition between two stages happens at strain about ~4–5, approximately corresponding to 4 ECAP passes (e = 4.6) or 2 passes with subsequent rolling (e = 4.9). Thus saturation of grain refinement happens at the same strain and boundary density for both ECAP and ECAP with subsequent cold rolling. Analysis of

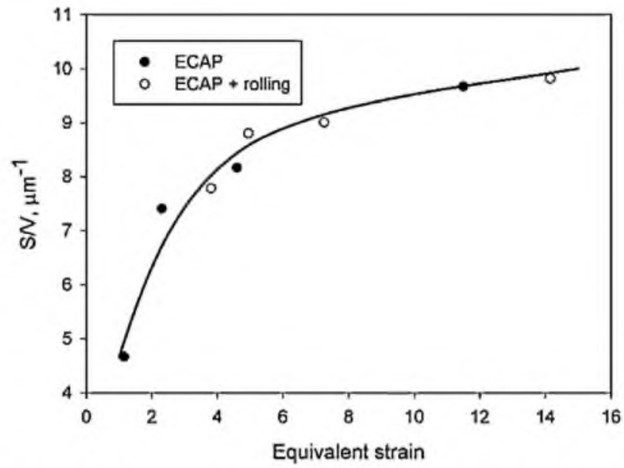

Fig. 8. Boundary density versus equivalent strain; calculated using TEM data.

increment in boundary density after rolling shows that noticeable grain refinement during rolling takes place after 1 pass. After 2 passes it is less pronounced, after 4 and 10 passes it almost does not take place. So, decrease in boundary spacing after rolling is caused only by geometrical effect of deformation after 4 and 10 passes.

However, there is one difference in microstructure of ECAPed specimens and rolled ones – significantly higher fraction of HABs after rolling – which could not be explained from a viewpoint of geometrical effect of strain. The increase in HABs is not proportional to increment of accumulated strain (Fig. 9), for example at comparable strain level (4 ECAP passes and 2 passes with rolling) HABs average fraction is equal to 23.9% and 35.2% respectively after ECAP and ECAP with rolling. The origins of the HABs fraction increase could be interconnected with specific mechanisms responsible for saturation of microstructure refinement at high strains.

Saturation of grain refinement is commonly observed in metals deformed at high strains. For copper, saturation was found after ECAP [14], HPT [24], multi-axial forging [26] and accumulative roll bonding [27] at room temperature. Saturation means a kind of steady-state process, so, generation of dislocations or other crystal lattice defects imposed by plastic deformation has to be balanced with some mechanisms of their annihilation. Commonly proposed way of realization of such balance is dynamic recovery/recrystallization mechanism. For multi-axial forging [26] and HPT [24] this phenomena was named differently, also, it occurred

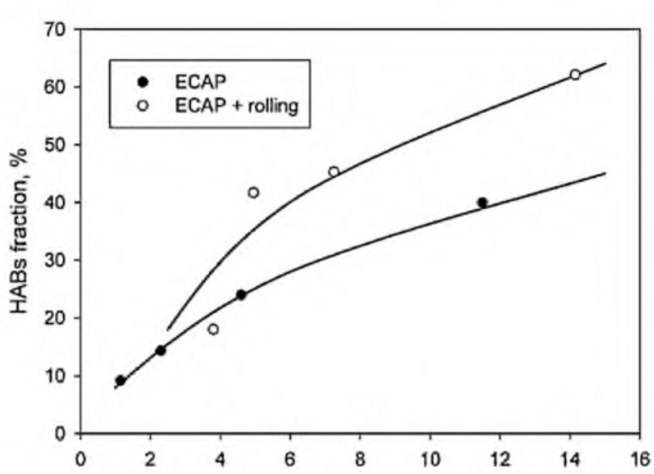

Fig. 9. Average HABs fraction versus equivalent strain.

at different strains, but the proposed mechanism involving boundaries migration was very similar. This mechanism resembled much conventional dynamic recrystallization. However, the exact mechanism is still unclear. Similar process could occur during ECAP. Such microstructural features, as relatively coarse recrystallized grains with thick sharp boundaries or recovered subgrains were found after ECAP in copper [15,18]. However, it is still a question as if these grains were formed during static or dynamic recrystallization [17]. Sometimes presence of such coarse grains was not found after deformation but they were found after room temperature storage [28]. One should also note that dynamic recovery was reported to occur after cold rolling of coarse-grained copper with reduction higher than 90% [29]. As a conclusion it is possible to state that microstructure development during deformation at saturation stage is associated with some recrystallization/recovery process. The rate of HABs formation is likely to be dependent on rate of this dynamic restoration process. So it could be suggested that higher fraction of HABs after rolling is due to more developed restoration process. But this suggestion needs verification.

To prove the assumption we carefully compared microstructure after 10 ECAP passes and 10 passes with subsequent rolling. Highest number of passes was chosen because restoration should be more developed at higher strain level and it would be easier to find corresponding microstructural features. As a measure of restoration misorientation across the line inside individual grain was chosen. Low misorientation means defect-free grain, most possibly recrystallized grain. Similar criterion was used in [30] to reveal recrystallized grains in copper and Cu–Zr alloy after ECAP. Misorientations ("point to origin misorientation") across the long axis of about 100 individual grains were analyzed. One plane (TD) was analyzed after ECAP; ND and TD planes were investigated after rolling. Volume distributions of grains according to their internal misorientation with average misorientation values are shown in Fig. 10.

Average misorientation is approximately 1.6 times lower after rolling (2.5–2.7°/μm versus 4.1°/μm). Also, volume fraction of grains with small misorientations inside them (less than 1°/μm) is higher after rolling (25–30% against 18%). Two types of grains with small misorientations inside them were found both after ECAP and rolling. First type of grains was very fine ones (≈0.1–0.2 μm) which could be to fine to have dislocation activity inside them. Second type ones were relatively coarse grains (up to ≈0.8 μm). After ECAP they are mostly rather equiaxed, after rolling they have much lower aspect ratio than average one – they are both thicker and shorter. Their orientation (indicated by their color on map) differed significantly from surrounding grains/subgrains. Defect free grains with low-aspect ratio were also found during TEM observations after rolling (Fig. 3). They are likely to originate from dynamic recrystallization. Dislocation density after 10 ECAP passes (examined on TD plane) was $3.3 \pm 1.2 \times 10^{14}\ m^{-2}$, after rolling it decreased to $1.6 \pm 0.7 \times 10^{14}\ m^{-2}$ – rolling resulted in twice lower dislocation density. So, as a summary, microstructural observations both by TEM and EBSD confirmed that rolling results in more restored microstructure in comparison to ECAP. This is likely to be the reason of higher HABs fraction after rolling. It is difficult to directly specify the reasons why rolling is more beneficial for dynamic restoration than ECAP. Possible reasons could be found in:

1) Difference in deformation conditions. For instance, strain rate could be estimated as $\sim 2 \times 10^{-1}\ s^{-1}$ and $\sim 5 \times 10^{-2}\ s^{-1}$ for ECAP and rolling respectively. The difference is not that high but still is about an order of magnitude. Lower strain rate could be beneficial for development of dynamic restoration process. Another difference is strain increment per pass. In case of ECAP each pass corresponds to strain equal to 1.15. Total rolling strain was 2.7 by 15–20 passes, which is equal to ~0.13–0.18 per pass. If

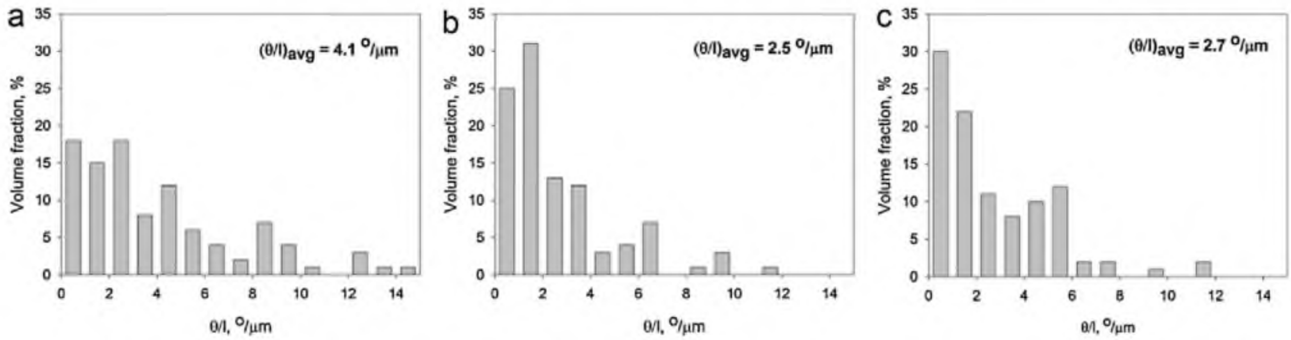

Fig. 10. Volume distribution of misorientation inside individual grains after 10 ECAP passes, TD (a), 10 ECAP passes and rolling, TD (b) and ND (c).

the restoration process is not dynamic but static (happens not during straining but between individual passes) like it was suggested in [28]; it possibly would also result in more restored microstructure. The temperature should also significantly affect restoration process; both ECAP and rolling were conducted at room temperature, but extensive deformation could give a rise to the temperature. Calculations showed that temperature rose to ≈50 °C during ECAP and to ≈30 °C during rolling. These values are significantly lower than usually reported temperature of onset of recrystallization in UFG copper (higher than 150 °C) [31], so it is unlikely that rise of temperature is enough to promote recrystallization.

2) Different character of microstructure, produced by ECAP and rolling. Microstructure after ECAP is close enough to equiaxed, but after rolling microstructure is lamellar, with high aspect ratio. It is known that lamellar structure tends to transform into equiaxed one due to surface tension in nodes where lamellar and intralamellar transversal boundaries intersect [32]. For example, both experimental studies and simulations of annealing behavior of UFG Al–Mg alloy with lamellar structure revealed that spheroidisation occurred before grain growth [33]. Thus it could be suggested that elongated structure would be less stable than equiaxed and so restoration process is likely to be more developed during rolling.

It was mentioned previously that rolling changes after ECAP texture dramatically. Texture has the potential to effect grain boundary distribution and thus fraction of HABs. Effect of texture on boundaries distribution could be estimated by comparison of correlated and uncorrelated grain boundary character distribution [34]. Both of them could be easily obtained from EBSD software. Correlated distribution is conventional distribution of misorientations measured along boundaries. Uncorrelated distribution is obtained by calculating misorientation between two arbitrary selected grains. In general, uncorrelated distribution considers misorientations derived from texture. Both correlated and uncorrelated distributions of HABs after 10 ECAP passes and subsequent rolling are shown in Fig. 11. Correlated and uncorrelated distributions are rather similar both after ECAP and rolling. Average misorientation could be used as a simple quantitive measure of these distributions. Uncorrelated distributions give very close average misorientations for ECAP and rolling – 40.6° and 40.8° respectively. Average misorientation values from correlated distributions are different – 38.2° after ECAP and 42.8° after rolling. Higher average misorientation after rolling correlates with higher fraction of HABs. The fact that average misorientations from uncorrelated distributions are similar clearly shows that texture does not affect HABs fraction.

4.2. Mechanical properties

Our data on mechanical properties for as-ECAPed copper correlates well with previous founding. Saturation of strength after 2–4 passes was commonly found for copper previously [10,11,14,16]. U.T.S saturation value about 400 MPa is in a good agreement with available data [9,14–16]. Higher values about 450 MPa were reported in case if back-pressure was used [10,11]. Strength of copper after ECAP and rolling exceeds typically reported strength (U.T.S. ≥ 400 MPa) of cold rolled copper [35]. Interesting fact is similarity of strength dependence on passes number between copper after ECAP and ECAP with subsequent rolling. This fact implies that

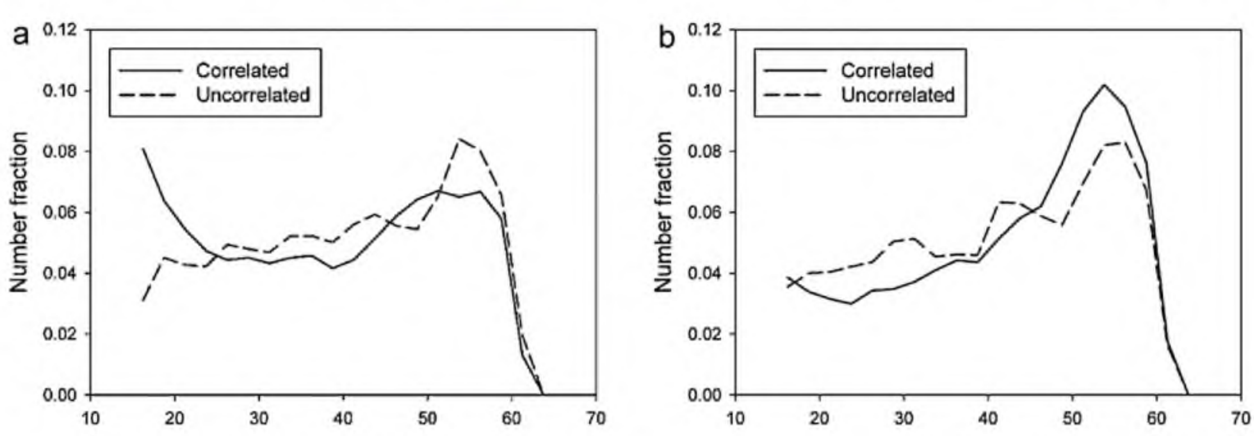

Fig. 11. Correlated and uncorrelated grain boundary character distributions calculated from EBSD data (TD plane); a – 10 ECAP passes; b – 10 ECAP passes with subsequent cold rolling.

despite major structure transformation during rolling mechanical properties are somehow inherited from ECAPed specimens. This could be expected from Fig. 8 demonstrating that strain has accumulative effect on boundary density.

Superior strength of UFG materials usually is ascribed to fine grain size using Hall–Petch (H–P) relationship between strength and grain size. Precise analysis for as-ECAPed copper [11] demonstrated that classical H–P relationship validates well if subgrain size was used. Misorientation of boundaries which could be introduced using modified H–P relationship [23] had minor importance. It means that strength increases due to formation of LABs, and further straining resulting in HABs fraction increase has negligible effect on strength. This explains well evolution of strength during ECAP. However, as it was shown previously, rolling does not result in further grain refinement in terms of new boundary formation after 4 and 10 ECAP passes. But relatively equiaxed grains/subgrains formed after ECAP became flattened after rolling, thus boundary spacing decreased on RD/TD planes. In order to evaluate validity of H–P relationship using boundary spacing on different planes the H–P plot is shown in Fig. 12 (boundary spacing were taken from TEM data).

As it was expected good correlation between yield strength and boundary spacing on all three planes were found after ECAP. After rolling H–P relationship validates if spacing on RD or TD were used. It means that strength is controlled by lamellae boundary distance after rolling. As it was mentioned previously these boundaries are GNBs and they might be more effective obstacles for dislocations than transversal IDBs (however, as it was mentioned previously, that does not imply their high-angle misorientation). The value of k about 142 MPa $\mu m^{-0.5}$ is relatively close to typical value for coarse-grained copper equal to 110 MPa $\mu m^{-0.5}$ [36]. Value of σ_0 of 36.4 MPa also corresponds rather well with typical value of 25 MPa.

It is interesting to note that not only strength is higher but ductility also increases as a result of rolling after 4 and 10 ECAP passes. This is quite an unexpected matter. One of the most commonly discussed possibilities to increase elongation is to increase strain hardening capability [37]. But values of Y.S. and U.T.S. are much closer after rolling than after ECAP, as it is shown in Table 2. This is indirect evidence of higher strain hardening capability after ECAP. Comparison of stress–strain curves after 10 passes ECAP and 10 passes with subsequent rolling prove this assumption (Fig. 7). But rather pronounced stage of steady-state like flow was observed after rolling, when flow stress remains almost constant after reaching its maximum values. Such a stage was nearly absent after ECAP. This kind of steady-state stage was also found after 4 ECAP passes and rolling, i.e. it is present when elongation is higher after rolling than after ECAP. Steady-state flow involves some kind of balance between creation and annihilation of defects, which results in constant flow stress. It is worth to note that similar process is responsible for saturation of fragmentation during ECAP and rolling. As stress state during uniaxial tension testing is relatively close to those during rolling, it is possible that the same process of dynamic restoration occurs and results in steady state flow in samples after 4 and 10 ECAP passes and rolling. After ECAP restoration process is unlikely to take place as deformation conditions during pressing and tension are distinctively different. Also restoration process itself is less developed during ECAP than during rolling as it was discussed previously. So the occurrence of restoration process similar to those operating during rolling could result in steady state flow and higher ductility of samples after 4 and 10 ECAP passes and consecutive rolling.

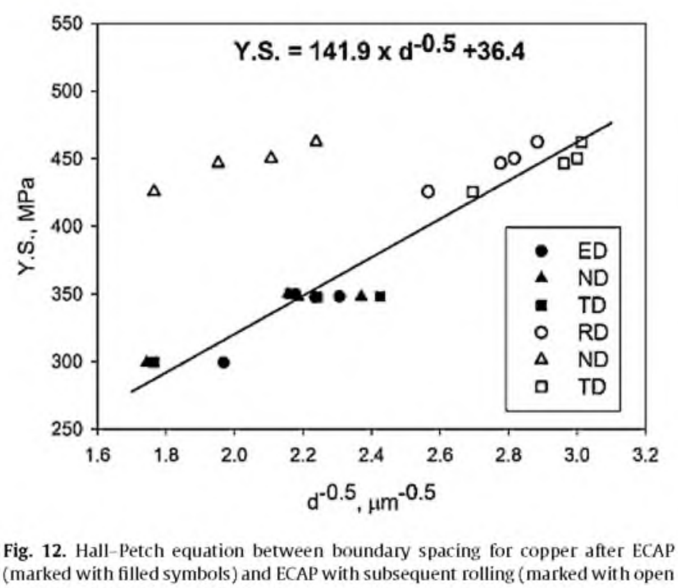

Fig. 12. Hall–Petch equation between boundary spacing for copper after ECAP (marked with filled symbols) and ECAP with subsequent rolling (marked with open symbols) and yield strength. (Y.S.)

5. Conclusions

Microstructure and mechanical properties of pure copper after 1–10 ECAP passes and ECAP with subsequent cold rolling with 90% cold rolling were compared. Following conclusions were made:

1) Rolling caused transformation of relatively equiaxed fine-grained structure formed in copper after ECAP into lamellar structure with even finer boundary spacing. For example, boundary spacing approaching 180 nm after 10 ECAP passes decreased to 110 nm after rolling. Transformation of equiaxed structure into lamellar is caused by geometrical requirements of strain, i.e. existing grains/subgrains changed their shape. Grain refinement in terms of formation of new boundaries was negligible during rolling of as-ECAPed copper.
2) Rolling after ECAP with corresponding number of passes caused significant increase (~20%) in average fraction of HABs. Growth of population of HABs was associated with pronounced dynamic restoration process, resulting in formation of defect-free grains with high misorientations.
3) Strength considerably increased (Y.S by more than 100 MPa) after rolling because of decrease in boundary spacing in accordance with Hall–Petch relationship.

Acknowledgments

The authors would like to express their gratitude to Dr. A. Zhilyaev and Dr. A. Belyakov for useful discussions and to Ms. J. Esina and Mr. E. Kudryavtsev for their help in TEM specimen preparation and observations. This work was supported by Russian Ministry of Science and Education under grant no. 14.740.11.0849.

References

[1] R.Z. Valiev, Y. Estrin, Z. Horita, T.G. Langdon, M.J. Zehetbauer, Y.T. Zhu, JOM 58 (2006) 33–39.
[2] R.Z. Valiev, T.G. Langdon, Prog. Mater. Sci. 51 (2006) 881–981.
[3] A.P. Zhilyaev, T.G. Langdon, Prog. Mater. Sci. 53 (2008) 893–979.
[4] R. Pippan, S. Scheriau, A. Taylor, M. Hafok, A. Hohenwarter, A. Bachmaier, Annu. Rev. Mater. Res. 40 (2010) 319–343.
[5] O.V. Mishin, G. Gottstein, Philos. Mag. A 78 (1998) 373–388.
[6] Y.G. Ko, S. Namgung, B.U. Lee, D.H. Shin, J. Alloys Compd. 504S (2010) S448–S451.
[7] K.X. Wei, W. We, Fei Wang, Q.B. Du, I.V. Alexandrov, J. Hu, Mater. Sci. Eng. A 528 (2011) 1478–1484.
[8] H. Akamatsu, T. Fujinami, Z. Horita, T.G. Langdon, Scripta Mater. 44 (2001) 759–764.
[9] Y. Huang, P.B. Prangnell, Acta mater. 56 (2008) 1619–1632.
[10] A.A. Almajid, E.A. El-Danaf, M.S. Soliman, J. Mater. Sci. 44 (2009) 5654–5661.
[11] E.A. El-Danaf, M.S. Soliman, A.A. Almajid, J. Mater. Sci. 46 (2011) 3291–3308.

[12] S.S. Hazra, A.A. Gazder, A. Carman, E.V. Pereloma, Metall. Mater. Trans. A 42 (2011) 1334–1348.
[13] V.V. Stolyarov, Y.T. Zhu, et al., Mater. Sci. Eng. A 343 (2003) 43–50.
[14] F. Dalla Torre, R. Lapovok, J. Sandlin, P.F. Thomson, C.H.J. Davies, E.V. Pereloma, Acta Mater. 52 (2004) 4819–4832.
[15] W.H. Huang, C.Y. Yu, P.W. Kao, C.P. Chang, Mater. Sci. Eng. A 366 (2004) 221–228.
[16] A. Mishra, B.K. Kad, F. Gregory, M.A. Meyers, Acta Mater. 55 (2007) 13–28.
[17] F.H. Dalla Torre, A.A. Gadzer, et al., J. Mater. Sci. 42 (2007) 9097–9111.
[18] F.H. Dalla Torre, A.A. Gadzer, et al., Metall. Mater. Trans. A 38 (2007) 1080–1095.
[19] I. Beyerlien, L. Toth, Prog. Mater. Sci. 54 (2009) 427–510.
[20] A. Gholinia, P.B. Prangnell, M.V. Markushev, Acta Mater. 48 (2000) 1115–1130.
[21] P.B. Prangnell, J.R. Bowen, A. Gholinia, in: A.R. Dineson, M. Eldrup, D. Juul Junsen, S. Linderoth (Eds.), Proc. of 22nd Riso Int. Symp. on Materials Science: Science of Metastable and Nanocrystalline Alloys – Structure, Properties and Modelling, Riso National Laboratory, Roskilde, Denmark, 2001, pp. 105–126.
[22] A.A. Gazder, W. Cao, C.H.J. Davies, E.V. Pereloma, Mater. Sci. Eng. A 497 (2008) 341–352.
[23] D.A. Hughes, N. Hansen, Acta Mater. 48 (2000) 2985–3004.
[24] T. Hebesberger, H.P. Stuwe, A. Vorhauer, F. Wetscher, R. Pippan, Acta Mater. 53 (2005) 393–402.
[25] J. Gil Sevillano, P. van Houtte, E. Aernoldt, Prog. Mater. Sci. 25 (1981) 69–412.
[26] A. Belyakov, T. Sakai, H. Muira, K. Tsuzaki, Philos. Mag. A 81 (2001) 2629–2643.
[27] N. Takata, S.-H. Lee, N. Tsuji, Mater. Lett. 63 (2009) 1757–1760.
[28] O.V. Mishin, A. Godfrey, Metall. Mater. Trans. A 39 (2009) 2923–2930.
[29] G.E. Truckner, D.E. Mikkola, Metall. Trans. A 8 (1997) 45–49.
[30] R. Kuzel, M. Janecek, Z. Matej, C. Cizek, M. Dopita, O. Srba, Metall. Mater. Trans. 41 (2010) 1174–1190.
[31] N. Lugo, N. Llorca, J.J. Sunol, J.M. Cabrera, J. Mater. Sci. 45 (2010) 2264–2273.
[32] F.J. Humphreys, M. Hatherly, Recrystallization, Related Annealing Phenomena, second ed., Elsevier Ltd, 2004.
[33] P.B. Prangnell, J.S. Hayes, J.R. Bowen, P.J. Apps, P.S. Bate, Acta Mater. 52 (2004) 3193–3206.
[34] T.R. McNelly, M.E. McMahon, Metall. Mater. Trans. A 28 (1997) 1879–1887.
[35] Y. Zhang, N.R. Tao, K. Lu, Acta Mater. 56 (2008) 2429–2490.
[36] W.F. Smith, J. Hashemi, Foundations of Materials Science and Engineering, fourth ed., McGraw-Hill, 2006.
[37] Y.M. Wang, E. Ma, Acta Mater. 52 (2004) 1699–1709.